OXFORD

Human Molecular Genetics, 2017, Vol. 26, No. 11 2034–2041

doi: 10.1093/hmg/ddx089
Advance Access Publication Date: 15 March 2017
Original Article

ORIGINAL ARTICLE

LRSAM1-mediated ubiquitylation is disrupted in axonal Charcot–Marie–Tooth disease 2P

Johanna E. Hakonen[1,2,3,†], Vincenzo Sorrentino[3,4,†], Rossella Avagliano Trezza[3,‡], Marit B. de Wissel[2], Marlene van den Berg[3], Boris Bleijlevens[3], Fred van Ruissen[2], Ben Distel[3,‡], Frank Baas[1], Noam Zelcer[3,*] and Marian A.J. Weterman[1,*]

[1]Department of Clinical Genetics, Leiden University Medical Center, Leiden, the Netherlands, [2]Laboratory of Genome Analysis, Department of Clinical Genetics, [3]Department of Medical Biochemistry, Academic Medical Center, University of Amsterdam, Meibergdreef 15, 1105AZ, Amsterdam and [4]Laboratory for integrative and systems physiology, EPFL, CH-1015, Lausanne, Switzerland

* To whom correspondence should be addressed. Tel: +31205665131; Email: n.zelcer@amc.uva.nl (N.Z.); Tel: +31 205664965; Email: m.a.j.weterman@lumc.nl, m.a.weterman@amc.uva.nl (M.A.J.W.)

Abstract

Charcot–Marie–Tooth (CMT) disease type 2 is a genetically heterogeneous group of inherited neuropathies characterized by motor and sensory deficits as a result of peripheral axonal degeneration. We recently reported a frameshift (FS) mutation in the Really Interesting New Gene finger (RING) domain of LRSAM1 (c.2121_2122dup, p.Leu708Argfs) that encodes an E3 ubiquitin ligase, as the cause of axonal-type CMT (CMT2P). However, the frequency of LRSAM1 mutations in CMT2 and the functional basis for their association with disease remains unknown. In this study, we evaluated LRSAM1 mutations in two large Dutch cohorts. In the first cohort ($n = 107$), we sequenced the full LRSAM1 coding exons in an unbiased fashion, and, in the second cohort ($n = 468$), we specifically sequenced the last, RING-encoding exon in individuals where other CMT-associated genes had been ruled out. We identified a novel LRSAM1 missense mutation (c.2120C > T, p.Pro707Leu) mapping to the RING domain. Based on our genetic analysis, the occurrence of pathogenic LRSAM1 mutations is estimated to be rare. Functional characterization of the FS, the identified missense mutation, as well as of another recently reported pathogenic missense mutation (c.2081G > A, p.Cys694Tyr), revealed that *in vitro* ubiquitylation activity was largely abrogated. We demonstrate that loss of the E2–E3 interaction that is an essential prerequisite for supporting ubiquitylation of target substrates, underlies this reduced ubiquitylation capacity. In contrast, LRSAM1 dimerization and interaction with the *bona fide* target TSG101 were not disrupted. In conclusion, our study provides further support for the role of LRSAM1 in CMT and identifies LRSAM1-mediated ubiquitylation as a common determinant of disease-associated LRSAM1 mutations.

[†]These authors contributed equally to the study.
[‡]Present address: Department of Neuroscience, Erasmus MC, Wytemaweg 80, Rotterdam 3015 CN, The Netherlands.
Received: February 13, 2017. **Revised:** March 2, 2017. **Accepted:** March 6, 2017

Introduction

Charcot–Marie–Tooth (CMT) disease is a group of common hereditary polyneuropathies with a frequency of occurrence estimated at 1:3300 in the general population (1). CMT is characterized by progressive and length-dependent loss of peripheral nerves leading to muscle weakness and/or sensory loss in distal limbs (2). It is a highly heterogeneous disease, both clinically and genetically, but can be grossly divided into two major forms based on electrophysiological nerve-conduction studies in patients (3,4). The most common form of CMT is the autosomal dominant demyelinating neuropathy (CMT1), which is defined by reduced nerve conduction velocities (NCVs) (5,6). Multiple genes have been associated with this form of CMT, and at large are implicated in myelination or neurodevelopment (7). The second CMT form, CMT2, is an axonal neuropathy characterized by nearly normal NCVs, but reduced nerve conduction amplitudes (6) suggesting that the defect is primary axonal. In addition to their clinical distinction, the two CMTs differ in their underlying genetic cause and, in contrast to CMT1, many CMT2-linked genes are not specifically associated with neural functions. As such, elucidating the function of CMT2-associated genes is a necessary first step in order to understand the mechanism behind this type of the disease.

Recent studies by our group, and others, have implicated mutations in *LRSAM1* in CMT2 (8–13). The *LRSAM1* gene is highly expressed in spinal cord motor neurons and encodes an E3 ubiquitin ligase that has been implicated in endocytosis, viral budding and clearance of intracellular bacteria by autophagy (8,14,15). Intriguingly, *LRSAM1* mutations have been linked to both dominant and recessive forms of CMT2. A recessive form has been reported in a Canadian family as a result of a homozygous mutation in the penultimate *LRSAM1* exon leading to a complete absence of the protein (9). We previously reported a dominant autosomal form due to a frameshift (FS) mutation in *LRSAM1* mapping to the C-terminal Really Interesting New Gene finger (RING) domain of the protein (8), a finding that was independently confirmed by two additional studies (9,10). This domain, found in other E3 ubiquitin ligases, is required for both E3 dimerization and ubiquitylation, which is a common post-transcriptional modification that plays a role in a diverse cellular process (16). Ubiquitylation requires the sequential activity of an E1 activating enzyme, E2 conjugating enzyme and E3 ligase and is subject to spatiotemporal regulation (17). Clustering of the disease-associated mutations to the RING domain points toward the E3 ubiquitin ligase activity of LRSAM1 as being an important determinant of its involvement in CMT2. However, the frequency of *LRSAM1* RING mutations in CMT patients and their functional consequences are unknown. To address these issues, we investigated the frequency of *LRSAM1* mutations in a Dutch CMT cohort and functionally characterized the consequence of RING mutations on LRSAM1 activity. Here, we report a novel pathogenic *LRSAM1* missense mutation and provide a functional basis for the association of LRSAM1 RING mutations with CMT2.

Results

Identification of a novel missense LRSAM1 mutation associated with CMT2

We recently identified a dominant pathogenic mutation in the *LRSAM1* gene in a large CMT2-family (8). Following our finding, several other groups recently reported additional dominant CMT-associated mutations in *LRSAM1* (9,12,13). Remarkably, all these

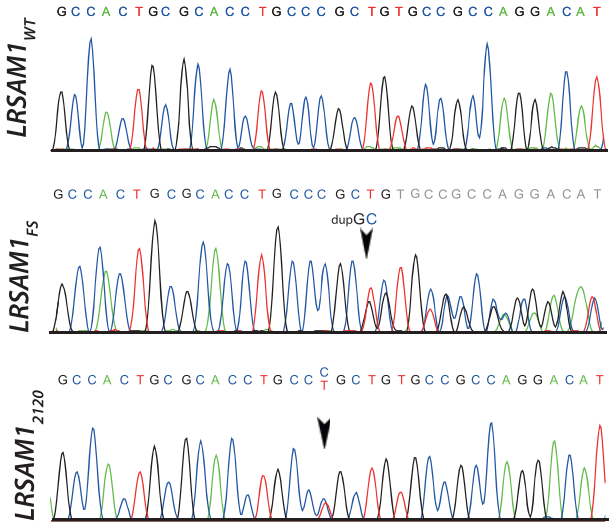

Figure 1. Identification of *LRSAM1* mutations in CMT2 patients. Sanger sequencing of genomic DNA of CMT patients ($n = 468$) revealed two mutations in exon 25 of *LRSAM1*; c.2121_2122dup and c.2120C > T. The previously described mutation c.2121_2122dup ($LRSAM1_{FS}$) is caused by an insertion of 2 base pairs and results a frame shift. In c.2120C > T ($LRSAM1_{2120}$), a single base pair change is observed which is predicted to be pathogenic. Arrows indicate the mutation site.

mutations map to the C-terminal RING structure of LRSAM1. To extend our initial finding and to assess the frequency of *LRSAM1* mutations in CMT, we screened a large Dutch cohort. Targeted sequencing of the complete *LRSAM1* coding sequence after a custom-made CMT capture of 107 samples did not yield pathogenic mutations. Only two variants were found which were reported as rare polymorphisms (rs150344223; rs149540339). Subsequently, in view of the concentration of reported *LRSAM1* mutations in the RING domain, we decided to specifically screen the RING-encoding exon of *LRSAM1* (NM_138361.5; exon 25) in a cohort of 468 patients by Sanger sequencing, in which we had ruled out mutations in the most prevalent CMT-associated genes. Two different mutations were identified (Fig. 1), one of which was the same FS mutation (c.2122_2123dup) as we described previously (8). This patient turned out to belong to the same family described in our initial report. We also identified a novel *LRSAM1* missense mutation (c.2120C > T; p.Pro707Leu) that is predicted to be pathogenic by Polyphen and SIFT accessed through the Alamut software package (Alamut Visual 2.7 ref 2, Interactive Software, Rouen, France). Based on EMG data, the patient carrying this mutation was diagnosed with an axonal type of CMT affecting both sensory and motor nerves. The age of onset was 50 years. There was no known consanguinity and the patient's sibling was also affected suggesting an autosomal dominant mode of inheritance. Unfortunately, DNA from other family members was not available for further analysis. Additionally, we detected common variants at frequencies comparable to those reported for the general population (5 and 2 out of 936 chromosomes for rs200242834 and rs549468112, respectively). Thus, our genetic analysis indicates that the occurrence of pathogenic *LRSAM1* mutations is a rather rare event (2 out of 468 in CMT cases for which the major CMT2 genes were already excluded).

RING-mediated dimerization is maintained in mutant LRSAM1

The RING domain is a central determinant of E3 ubiquitin ligase function (16,21). Structural studies highlight the important role

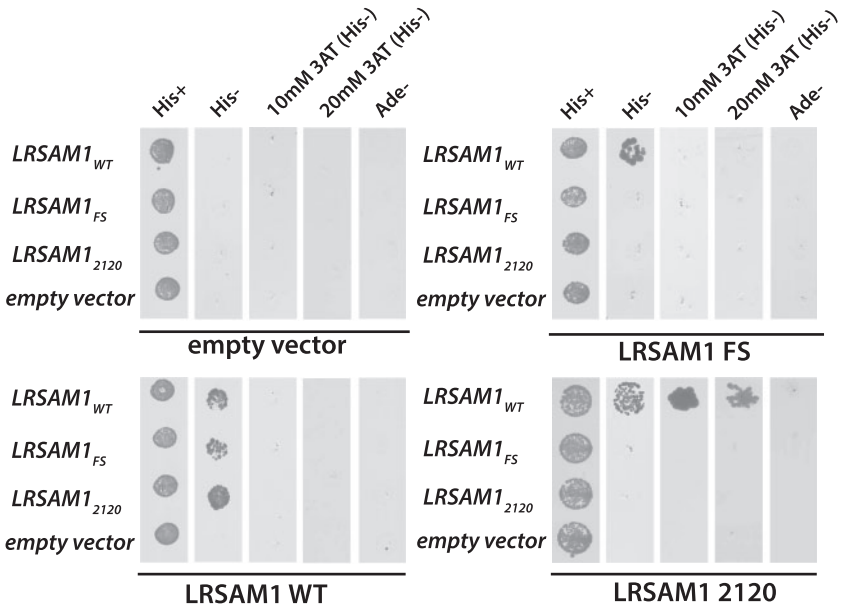

Figure 2. A CMT-associated mutation in the RING domain of *LRSAM1* does not impair dimerization. Wild type and the CMT-associated LRSAM1 RING mutants (c.2121_2122dup and c.2120C > T). LRSAM1 were cloned into yeast-2-hybrid prey and bait plasmids as indicated. Transformed haploid yeast were mated and diploid cells were serially diluted and plated on selective medium (-HIS, -ADE). An image from the first serial dilution (10^5 diploid cells plated) is shown. Results are representative of three biological replicates. 3AT (3-amino-1,2,4-triazole) serves as an indicator of interaction strength.

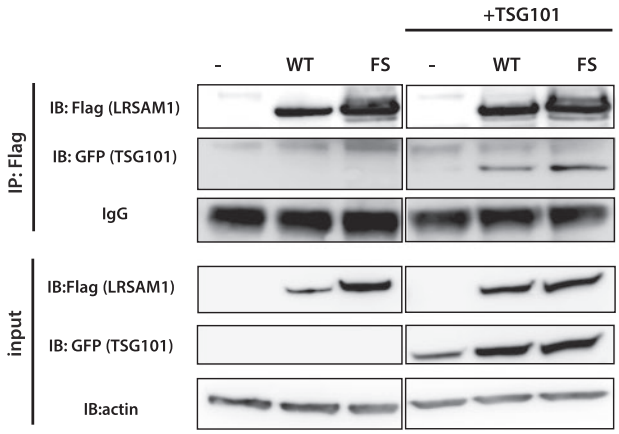

Figure 3. A CMT-associated mutation in the RING domain of *LRSAM1* does not impair the interaction between LRSAM1 and TSG101. HEK293T cells were transfected with the indicated FLAG-LRSAM1 and GFP-TSG101 expression plasmids at a 1:1 ratio. After 48 h, cells were harvested, lysed and subsequently, samples were immunoblotted and analyzed as indicated. Immunoblots shown are representative of three independent experiments. Bands shown were obtained from the same blot. WT, wild type; FS, CMT-associated LRSAM1 RING mutation (c.2121_2122*dup*).

of the RING domain in coordinating dimerization of RING-containing E3 ligases, a step often required for their function. Disruption of dimerization may lead to impaired E3 ligase activity and loss of interaction with E2 enzymes (21). We, therefore, reasoned that the CMT-associated *LRSAM1* mutations could disturb dimerization. To test this notion, we compared wild-type (WT) LRSAM1, with the previously reported FS mutation, our novel missense mutation and another recently reported pathogenic missense *LRSAM1* RING mutation in a yeast-2-hybrid (Y2H) assay (Fig. 2). In line with the general tendency of RING E3 ligases to dimerize, we found that WT LRSAM1 can form homodimers in this assay. We observed that this interaction was also maintained between the WT and the CMT-associated LRSAM1 RING mutants, suggesting that disrupted dimerization is unlikely to underlie the pathogenic consequence of this mutation.

A CMT-associated RING mutation does not affect the interaction of LRSAM1 with TSG101

TSG101 is among the few validated targets of LRSAM1 reported to date (14). We previously demonstrated that unlike WT LRSAM1, the CMT-associated FS mutant LRSAM1 was not able to decrease abundance of exogenously introduced TSG101, akin to an LRSAM1 mutant with an engineered disrupted RING (8). Therefore, having ruled out dimerization, we considered the possibility that the CMT-associated mutations alter the ability of LRSAM1 to interact with its ubiquitylation targets. To test this, we performed co-immunoprecipitation studies in mammalian HEK293T cells (Fig. 3). As anticipated, WT LRSAM1 readily interacted with TSG101. The LRSAM1 FS mutant with an altered RING domain also showed interaction with TSG101, indicating that the interaction of LRSAM1 and TSG101 is not affected by disruption of the RING.

RING mutations abolish the interaction with the E2 conjugating enzyme UBC13

In addition to supporting dimerization, the RING domain acts also as a scaffold for recruitment of E2 ubiquitin-conjugating enzymes and thereby facilitating conjugation of activated ubiquitin to target proteins. We tested whether the CMT-associated RING mutations could affect the interaction with E2 enzymes and consequently, impair the ubiquitylation capacity of LRSAM1. We used the Y2H approach to screen for the interaction between the WT LRSAM1 or the three CMT-associated LRSAM1 RING mutants (c.2121_2122dup, c.2120C > T and

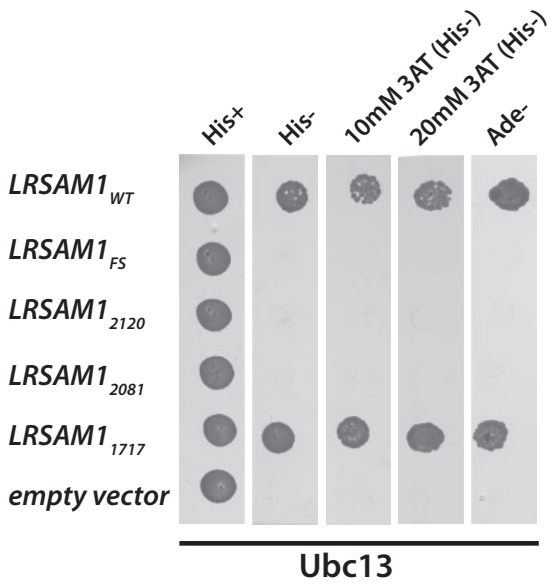

Figure 4. Interaction with the E2 ubiquitin-conjugating enzyme UBC13 is lost in CMT-associated LRSAM1 mutants. Wild-type (WT) or CMT-associated *LRSAM1* mutant constructs were used as "bait" in a yeast-two-hybrid assay together with the E2 ubiquitin enzyme UBC13 ("prey"). A strong interaction with UBC13 was observed with $LRSAM1_{WT}$ and $LRSAM1_{1717}$, but not with the CMT-associated LRSAM1 mutations $LRSAM1_{2120}$, $LRSAM1_{2081}$ and $LRSAM1_{FS}$. An image from the first serial dilution (10^5 diploid cells plated per condition) is shown and results are representative of two biological replicates. LRSAM1 wild type, $LRSAM1_{WT}$; $LRSAM1_{1717}$, LRSAM1 polymorphism (c.1717C > A); $LRSAM1_{FS}$, LRSAM1 RING mutation (c.2121_2122dup); $LRSAM1_{2120}$, LRSAM1 RING mutation (c.2120C > T); $LRSAM1_{2081}$, LRSAM1 RING mutation (c.2081G > A); 3AT (3-amino-1,2,4-triazole).

c.2081G > A) with the E2 enzyme UBC13, an E2 enzyme that is specifically implicated in generation of K63-polyubiquitin chains (22) and reported to interact with LRSAM1 (23–25). In this experiment, we also included a non-pathogenic *LRSAM1* variant (c.1717C > A) (rs150882646) that serves as an additional control. Consistent with published results, we were able to confirm the interaction between UBC13 and WT LRSAM1. This interaction occurred in the context of both the full-length LRSAM1 protein (Fig. 4), as well as in the context of the RING domain only (not shown), in agreement with the accepted notion that the RING domain mediates the interaction between E2 and E3. As anticipated, the protein encoded by the polymorphic variant (c.1717C > A) also interacted with UBC13 similar to WT LRSAM1. However, the interaction with UBC13 was lost with all three CMT-associated LRSAM1 mutants (Fig. 4). This result demonstrates that pathogenic mutations affecting the RING of LRSAM1 have a functional consequence and that the loss of interaction with a cognate E2 enzyme, and hence target ubiquitylation, may form an important aspect of the disease mechanism.

Ubiquitylation is impaired in CMT-associated LRSAM1 RING mutants

Since an intact E2–E3 interaction is a prerequisite for target-protein ubiquitylation, we reasoned that LRSAM1 RING mutants would have impaired ubiquitylation activity. To test this hypothesis, we generated recombinant LRSAM1 RING proteins corresponding to the WT, FS mutant, and the two missense mutations c.2120C > T (2120) and c.2081G > A (2081) (Fig. 5). As expected, the FS corresponding RING protein had lower mobility in an SDS-PAGE gel, consistent with it being larger than the WT RING due to the 12 amino acid extension of the LRSAM1 C-terminus (8). We then tested the ability of the purified protein to stimulate ubiquitylation *in vitro* in conjunction with UBC13/UEV1a and UbcH5a, two E2 enzymes that have been reported to interact with LRSAM1 in global E2–E3 screens (23–25). In these *in vitro* assays, we could assess both the formation of unlinked poly-ubiquitin chains and the auto-ubiquitylation of LRSAM1 as detected by ubiquitylation of the RING protein itself. WT LRSAM1 facilitated robust, ATP-dependent formation of free poly-ubiquitin chains with both E2s (Fig. 5B). In contrast, this activity was abrogated when using the mutant RING proteins. The residual poly-ubiquitin chains that are formed with UBC13/EEV1a, also with the mutant RINGs, are a result of the intrinsic activity of this E2 and occur also when no RING is added in an ATP-dependent manner [data not shown (20)]. Furthermore, UBC5Ha, but not UBC13/UEV1a, could promote ATP-dependent auto-ubiquitylation of the WT LRSAM1 RING, an intrinsic RING-dependent activity that was not observed with the mutant RING proteins (Fig. 5B). As such, our results suggest that the CMT-associated RING mutations severely attenuate LRSAM1-stimulated ubiquitylation activity. Therefore, loss of target ubiquitylation may underlie the role of LRSAM1 in CMT development.

Discussion

LRSAM1 is one of the several genes recently identified to cause CMT2 (8,9). In this study, we set out to determine the frequency of *LRSAM1* mutations that contribute to CMT and in doing so, also to identify novel CMT-associated *LRSAM1* mutations. As is the case with other CMT2 genes, *LRSAM1* mutations proved to be rare. Direct sequencing of the last exon encoding the RING domain yielded a novel CMT-associated missense mutation, c.2120C > T (p.Pro707Leu), that is also one of the first reported missense mutations in *LRSAM1*. We show evidence demonstrating that CMT2-associated mutations impair the interaction between LRSAM1 and its cognate E2 enzyme, and that this results in severe loss of ubiquitylation activity. As such, our results point towards impaired LRSAM1-mediated ubiquitylation as the underlying disease mechanism

LRSAM1 is a member of the RING family of E3 ubiquitin ligases. To date, all reported autosomal dominant LRSAM1 mutations congregate in the RING domain; a domain present in RING E3 ligases that is essential for their dimerization and ubiquitylation activity (21,26,27). Furthermore, while our study was under review, two additional missense mutations in LRSAM1 were reported affecting the same amino-acid (p.Cys694 > Tyr, p.Cys694 > Arg) (12,13). Using several distinct experimental approaches, we evaluated the consequence of a panel of CMT2-associated RING mutations on LRSAM1 function. This allowed us to rule out disrupted LRSAM1 dimerization, and loss of interaction with the *bona fide* ubiquitylation target TSG101 as plausible explanations for the association of LRSAM1 with CMT2. The RING domain also mediates the interaction between the E2 and the E3 and three global Y2H screens investigating the E2–E3 interactome reported an interaction between LRSAM1 and the E2 enzymes UBC13 (UBE2N) and UbcH5A (UBE2D1) (23,24,28). Our study confirmed the interaction between WT LRSAM1 and UBC13, and further demonstrated that the CMT-associated mutations in *LRSAM1* ablated the interaction with UBC13, thus affecting a property of LRSAM1 that is crucial for efficient target ubiquitylation. Concordantly, we demonstrate that this strongly

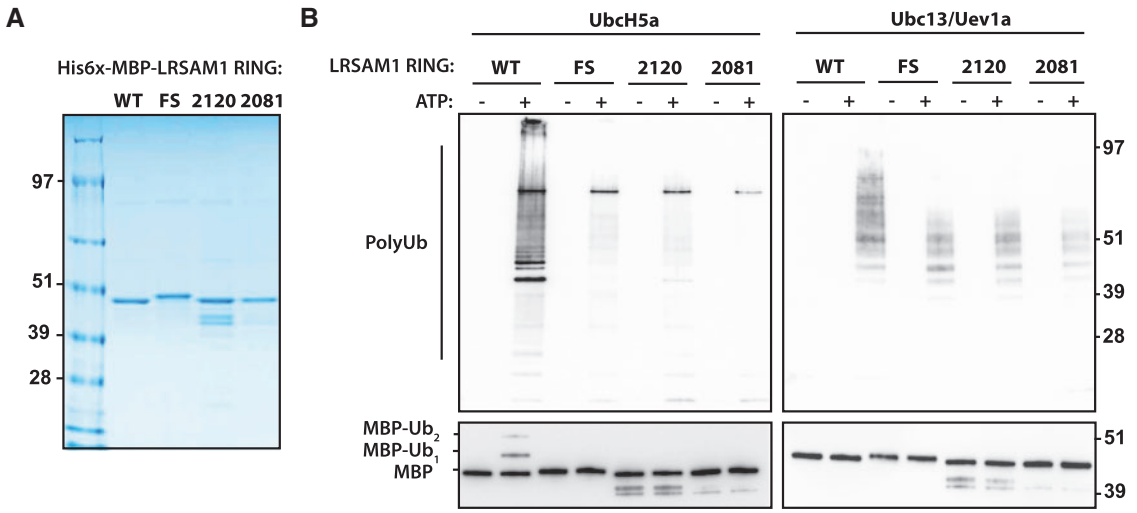

Figure 5. CMT-associated mutations in the LRSAM1 RING domain attenuate ubiquitin ligase activity. (**A**) Coomassie-stained SDS-PAGE gels with purified His6-MBP-tagged recombinant wild type (WT) and mutant LRSAM1 RING proteins (FS, 2120, 2081). Note that the frameshift (FS) RING migrates with lower mobility, consistent with it having a higher molecular weight as a result of a 12 amino acid extension. (**B**) *In vitro* ubiquitylation assay using the indicated LRSAM1 RINGs with the E2 enzymes UbcH5a or UBC13/UEV1a. Reactions were separated on SDS-PAGE gels and ubiquitin and the MBP-RING were detected by immunoblotting. A representative immunoblot from three independent experiments is shown. The poly-ubiquitin chains and the mono- and di-ubiquitylated MBP RING are indicated.

attenuates the ubiquitylation activity of the CMT-associated RING proteins *in vitro*. Ubiquitin is able to form different types of ubiquitin chains depending on the interacting E2 enzyme, thereby targeting the ubiquitylated protein to distinct cellular fates (29,30). Recent studies demonstrated that LRSAM1 can predominantly form K6, K27, K29 and K48 poly-ubiquitin chains with members of the UBE2D family of E2 enzymes (15,31). With this in mind, it is interesting to point out that UBC13, with which LRSAM1 interacts, has been specifically reported to generate K63-linked ubiquitin chains that are implicated in non-proteolytic signaling and trafficking (22,32). As such, our results expand the repertoire of ubiquitin linkages that LRSAM1 facilitates. Future studies are needed to determine the global landscape of LRSAM1 ubiquitylation targets.

Interestingly, LRSAM1 has been associated with both dominant and recessive forms of CMT (9). While no protein could be detected in the lymphocytes of a patient carrying the homozygous recessive mutation, patients with autosomal-dominant mutations retain an unaffected WT allele (9). Dimerization of WT LRSAM1 with mutant LRSAM1, both of which are present in patients carrying a heterozygous dominant mutation, was not affected. However, the mutant proteins were not able to form homodimers, which may partially contribute to the pathogenic phenotype. Since the patients with the recessive loss of function mutations and dominant cases have a similar clinical phenotype, the dominant mutation most probably exerts its effect in a dominant-negative manner. Heterodimers composed of WT and mutant LRSAM1 may be non-functional and, therefore, point towards a loss-of-function mechanism. Alternatively, mutant LRSAM1 may have altered function or binding partners resulting in toxic gain-of-function. These possibilities do not rule out other LRSAM1-dependent mechanisms. Indeed, two recent reports suggest that LRSAM1 RING mutants influence gene expression, potentially as a result of an altered interaction with RNA binding proteins (12,13). Moreover, our preliminary results suggest that CMT2-associated LRSAM1 variants have the propensity to form aggregates in cells (data not shown), offering an additional mechanism by which these mutations can contribute to CMT2.

Our results are in line with the emerging importance of ubiquitylation as a post-translational modification in neurological disease. In addition to LRSAM1, other E3 ubiquitin ligases have been reported to play a role in neurodegenerative diseases. TRIM2, also a member of the RING E3 ubiquitin family, was recently implicated in early-onset axonal neuropathy in which altered TRIM2-mediated ubiquitylation resulted in axonal degradation (33). In addition to its involvement in CMT, LRSAM1 was reported as a potential modifier of Huntington's disease owing to its ability to regulate localization and clearance of the Htt protein (34). Another well-known E3 ligase, Parkin, is associated with familial Parkinson's disease (35–37). Intriguingly, Parkin is reported to associate with UBC13 and to stimulate K63-linked poly-ubiquitylation formation (38). Coincidently, three patients of the original family in which we identified the frame shift mutation in *LRSAM1* developed Parkinson's disease later in life (39), suggesting a broader role for LRSAM1 in neurodegenerative diseases.

Taken together, our results indicate that LRSAM1-mediated ubiquitylation is relevant for the etiology of CMT2. Future studies aimed at identification of LRSAM1 ubiquitylation targets and interacting proteins are necessary to obtain a comprehensive view of the changes that ultimately lead to CMT. While next generation sequencing techniques have accelerated discovery of disease-associated variants, development of functional assays has lagged behind. We provide here a functional assay to test RING domain LRSAM1 mutants. Finally, we propose that the role of LRSAM1 may extend beyond peripheral neurologic disease, warranting further investigation into its role in neurodegenerative diseases affecting the central nervous system. Whether the mechanisms linking LRSAM1 to CMT2 and these other diseases are shared remains to be determined.

Materials and Methods

DNA samples and sequencing

All DNA samples were obtained with patient's consent. Genomic DNA was isolated from blood using standard

procedures. For the targeted sequencing, 1 μg of genomic DNA was used for preparing a sequencing library that was pre-amplified for 8 cycles. Subsequently, 1 μg of pre-amplified libraries of 6–14 patients was used for one CMT capture according to the procedure described by Nimblegen. The custom-made CMT-specific capture (Nimblegen, Roche) which was developed for diagnostic screening of peripheral neuropathies and included the coding parts of *LRSAM1* was followed by sequencing with the miSeq V2 kit on an Illumina miSeq sequencer. Alignment and re-alignment were performed using HG19 and BWAMEM.0.7.8. For variant calling, GATK-2.8-1-g932cd3a was used. Variants were callable when meeting all quality criteria we have for this procedure (i.e. coverage of at least 30× with both base and mapping quality ≥20). Non-callable positions or regions were filled in by Sanger sequence analysis. For direct Sanger sequencing of the RING-containing exon (exon 25 of *LRSAM1;* NM_138361.5) samples from 468 CMT patients without pathogenic mutation in *MPZ, GJB1, PMP22, RAB7A, LITAF, EGR2, HSPB1, GARS, MFN2, BSCL2, SH3TC2, DMN1, LMNA, CTDP1, NDRG1* and *GDAP1* were included. For amplification, 20 ng of genomic DNA was used as template in a PCR reaction with exon 25-specific M13-tagged primers (M13exon25-FWD 5′-TGTAAAACGACGGCCAGTGTAGGG CCAGCCACATGC-3′ and M13exon25-REV 5′-CAGGAAACAGCTA TGACCGCAGCAGATCCGTGATTAGG-3′) and Hotfire polymerase (Solys Biodyne), according to the manufacturer's protocol. The amplified PCR products were treated with shrimp alkaline phosphatase and exonuclease I prior to sequencing using the Big Dye Terminator cycle-sequencing kit and M13 primers on an ABI3730xl sequencer (Thermo Scientific). DNA sequences were analyzed with CodonCode Aligner (CodonCode Corporation, Centerville, MA, USA) and Alamut Visual 2.7 ref 2 (Interactive Software, Rouen, France).

Plasmids and expression constructs

Expression plasmids for FLAG tagged full-length WT, FS LRSAM1 mutant, and GFP-TSG101 were reported previously (8,18). The WT LRSAM1 RING was amplified from the full-length WT *LRSAM1* expression plasmid (8) and inserted into the bacterial expression plasmid His_6-MBP-DEST (a kind gift of Dr D. Waugh, NCI) using gateway cloning. The RING missense constructs were generated by site-directed mutagenesis using the QuickChange II XL kit (Agilent Technologies) and WT RING construct as a template. The FS LRSAM1 RING was generated as above, but with a full-length FS *LRSAM1* expression plasmid as template (8). All RING constructs started at codon 1995 of the *LRSAM1* coding sequence (corresponding to amino acid 665). The FS results in an alternative stop codon, which extends the protein by 12 amino acids beyond the native stop codon. For the Y2H assays, WT or mutated *LRSAM1* (c.2121_2122dup, c.2120C > T, c.1717C > A, c.2081G > A) were cloned into pACT2-DEST or pGDBU-DEST with Gateway recombination. The pGDBU-UBC13 plasmid was described previously (19).

Purification of recombinant LRSAM1 RING domain expressed in *Escherichia coli*

His_6-MBP-tagged LRSAM1 RING proteins were produced in the bacterial RIPL strain (Novagen). Bacteria were grown in LB at 37 °C to an A_{600} of 0.6 and induced with 1 mM isopropyl 1-thio-β-d-galactopyranoside for 4 h. Bacterial pellets were collected, lysed in lysis buffer (50 mM Tris-HCl, pH 7.6, 0.5 M NaCl, 5 mM imidazole and 1 mM DTT) supplemented with protease inhibitors and subsequently sonicated on ice to disrupt cellular integrity. Cell debris was removed by centrifugation and lysates loaded onto HisTrap HP columns (GE Healthcare) coupled to a cooled (4 °C) NGC Quest 10 Plus purification system (Bio-Rad). Bound proteins were eluted with imidazole, desalted using HiTrap desalting columns (GE Healthcare), and collected in elution buffer (20 mM Tris-HCl, pH 7.6, 100 mM NaCl, 1 mM DTT). Aliquots were frozen in liquid N_2 and stored at −80 °C.

In vitro ubiquitylation assay

Recombinant rabbit E1, UBCH5a, UBC13 and UEV1a were described previously (20). Briefly, reactions were carried out at 37 °C for 2 h in 20μl reactions containing 25 mM Tris, pH 8, 100 mM NaCl, 5 mM $MgCl_2$, 1 mM DTT and the following as indicated: 5 mM ATP, 0.4 μg of recombinant rabbit E1, 0.4 μg of UBCH5a or UBC13 and UEV1a, 2.5 μg of ubiquitin (Biomol), and 1 μg of LRSAM1 RING. Reactions were stopped by the addition of SDS-PAGE loading buffer and subjected to immunoblotting as described.

Y2H assay

The *Saccharomyces cerevisiae* strains used in this study were PJ69-4a (trp1-901 leu2-3,112 ura3-52 his3-200 gal4D gal80D LYS2::GAL1-HIS3 GAL2-ADE2 met2::GAL7-lacZ) and PJ69-4α (trp1-901 leu2-3,112 ura3-52 his3-200 gal4D gal80D LYS2::GAL1-HIS3 GAL2-ADE2 met2::GAL7-lacZ). PJ69-4a cells were transformed with pACT2-DEST encoding WT or mutant *LRSAM1*, while PJ69-4α cells were transformed with the indicated pGDBU-DEST constructs. Culturing conditions and Y2H assay protocol have been described previously (19). 3-AT is a competitive inhibitor of the *HIS3* gene product and, therefore, increases the stringency of the HIS- selection and is used as a strength indicator.

Cell culture and transfection

HEK293T cells were maintained in DMEM (Invitrogen) supplemented with 10% fetal bovine serum (FBS) (Gibco) and 10 000 U/mL Penicillin–Streptomycin (Sigma-Aldrich) at 37 °C and 5% CO_2. Transfection of the cells was carried out in 6-wells format with sub-confluent cells using JetPrime (Polyplus-transfection) according to the manufacturer's instructions. Transfection efficiency was monitored by co-transfection with an expression plasmid for GFP or mCherry and was consistently >85%.

Immunoblotting and co-immunoprecipitation

HEK293 cells were lysed in NP40 lysis buffer (Boston Bioproducts, Ashland, MA, USA) 48 h post-transfection. Total cell lysates were cleared by centrifugation at 1000*g* for 5 min at 4 °C. For co-immunoprecipitation, the lysates were incubated with 20 μL prewashed anti-Flag M2 affinity beads (Sigma-Aldrich) for 16 h at 4 °C. Subsequently, beads were washed four times with NP40 lysis buffer and immunoprecipitated protein eluted by boiling in SDS-PAGE loading buffer. Samples were separated by SDS-PAGE electrophoresis and transferred to a nitrocellulose membrane (Invitrogen) and probed as indicated with antibodies against Flag (M2, Sigma-Aldrich, 1:1000), GFP (Biolegend, 1:1000) ACTIN (Sigma-Aldrich, 1:1000) ubiquitin (FK2, Biomol, 1:1000) and MBP (clone 17, Sigma-Aldrich, 1:2000). Secondary horseradish peroxidase-

conjugated antibodies (Dako) were used and visualized with chemiluminescence on a Fuji LAS4000 (GE Healthcare). All immunoblots are representatives of at least two independent experiments.

Acknowledgements

We thank members of the Frank Baas lab, members of the Zelcer group and Irith Koster for their comments and suggestions on this manuscript.

Conflict of Interest statement. None declared.

Funding

This work was supported by the Prinses Beatrix Spierfonds (W.OR15). N.Z. is supported by an ERC Consolidator grant (617376) from the European Research Council and by Stichting Zabawas.

References

1. Pagon, R.A., Adam, M.P., Ardinger, H.H., Wallace, S.E., Amemiya, A., Bean, L.J., Bird, T.D., Ledbetter, N., Mefford, H.C., Smith, R.J., *et al*. (1993) *GeneReviews®* University of Washington, Seattle.
2. Harding, A.E. and Thomas, P.K. (1980) The clinical features of hereditary motor and sensory neuropathy types I and II. *Brain*, **103**, 259–280.
3. Dyck, P.J. and Lambert, E.H. (1968) lower motor and primary sensory neuron diseases with peroneal muscular atrophy. *Arch. Neurol.*, **18**, 619–625.
4. Thomas, P.K. and Calne, D.B. (1974) Motor nerve conduction velocity in peroneal muscular atrophy: evidence for genetic heterogeneity. *J. Neurol. Neurosurg. Psychiatry*, **37**, 68–75.
5. Krajewski, K.M., Lewis, R.A., Fuerst, D.R., Turansky, C., Hinderer, S.R., Garbern, J., Kamholz, J. and Shy, M.E. (2000) Neurological dysfunction and axonal degeneration in Charcot-Marie-Tooth disease type 1A. *Brain*, **123**, 1516–1527.
6. Bienfait, H.M.E., Verhamme, C., Schaik, I.N., Koelman, J.H.T.M., Visser, B.W.O., Haan, R.J., Baas, F., Engelen, B.G.M. and Visser, M. (2006) Comparison of CMT1A and CMT2: similarities and differences. *J. Neurol*, **253**, 1572–1580.
7. Gutmann, L. and Shy, M. (2015) Update on Charcot-Marie-Tooth disease. *Curr. Opin. Neurol.*, **28**, 462–467.
8. Weterman, M.A.J., Sorrentino, V., Kasher, P.R., Jakobs, M.E., van Engelen, B.G.M., Fluiter, K., de Wissel, M.B., Sizarov, A., Nürnberg, G., Nürnberg, P., *et al*. (2012) A frameshift mutation in LRSAM1 is responsible for a dominant hereditary polyneuropathy. *Hum. Mol. Genet.*, **21**, 358–370.
9. Guernsey, D.L., Jiang, H., Bedard, K., Evans, S.C., Ferguson, M., Matsuoka, M., Macgillivray, C., Nightingale, M., Perry, S., Rideout, A.L., *et al*. (2010) Mutation In The Gene Encoding Ubiquitin Ligase LRSAM1 in patients with Charcot-Marie-Tooth disease. *PLoS Genet.*, **6**, e1001081.
10. Nicolaou, P., Cianchetti, C., Minaidou, A., Marrosu, G., Zamba-Papanicolaou, E., Middleton, L. and Christodoulou, K. (2012) A novel LRSAM1 mutation is associated with autosomal dominant axonal Charcot-Marie-Tooth disease. *Eur. J. Hum. Genet.*, **21**, 190–194.
11. Engeholm, M., Sekler, J., Schöndorf, D.C., Arora, V., Schittenhelm, J., Biskup, S., Schell, C. and Gasser, T. (2014) A novel mutation in LRSAM1 causes axonal Charcot-Marie-Tooth disease with dominant inheritance. *BMC Neurol.*, **14**, 118.
12. Hu, B., Arpag, S., Zuchner, S. and Li, J. (2016) A novel missense mutation of CMT2P alters transcription machinery. *Ann. Neurol.*, 10.1002/ana.24776.
13. Peeters, K., Palaima, P., Pelayo-Negro, A.L., García, A., Gallardo, E., García-Barredo, R., Mateiu, L., Baets, J., Menten, B., De Vriendt, E., *et al*. (2016) Charcot-Marie-Tooth disease type 2G redefined by a novel mutation in *LRSAM1*. *Ann. Neurol.*, **80**, 823–833.
14. Amit, I., Yakir, L., Katz, M., Zwang, Y., Marmor, M.D., Citri, A., Shtiegman, K., Alroy, I., Tuvia, S., Reiss, Y., *et al*. (2004) Tal, a Tsg101-specific E3 ubiquitin ligase, regulates receptor endocytosis and retrovirus budding. *Genes Dev.*, **18**, 1737–1752.
15. Huett, A., Heath, R.J., Begun, J., Sassi, S.O., Baxt, L.A., Vyas, J.M., Goldberg, M.B. and Xavier, R.J. (2012) The LRR and RING domain protein LRSAM1 is an E3 ligase crucial for ubiquitin-dependent autophagy of intracellular *Salmonella typhimurium*. *Cell Host Microbe*, **12**, 778–790.
16. Metzger, M.B., Hristova, V.A. and Weissman, A.M. (2012) HECT and RING finger families of E3 ubiquitin ligases at a glance. *J. Cell Sci.*, **125**, 531–537.
17. Capili, A.D. and Lima, C.D. (2007) Taking it step by step: mechanistic insights from structural studies of ubiquitin/ubiquitin-like protein modification pathways. *Curr. Opin. Struct. Biol.*, **17**, 726–735.
18. Burgdorf, S., Leister, P. and Scheidtmann, K.H. (2004) TSG101 interacts with apoptosis-antagonizing transcription factor and enhances androgen receptor-mediated transcription by promoting its monoubiquitination. *J. Biol. Chem.*, **279**, 17524–17534.
19. Nelson, J.K., Sorrentino, V., Avagliano Trezza, R., Heride, C., Urbe, S., Distel, B. and Zelcer, N. (2016) The deubiquitylase USP2 regulates the LDLR pathway by counteracting the E3-ubiquitin ligase IDOLNovelty and significance. *Circ. Res.*, **118**, 410–419.
20. Sorrentino, V., Scheer, L., Santos, A., Reits, E., Bleijlevens, B. and Zelcer, N. (2011) Distinct functional domains contribute to degradation of the low density lipoprotein receptor (LDLR) by the E3 ubiquitin ligase inducible Degrader of the LDLR (IDOL). *J. Biol. Chem.*, **286**, 30190–30199.
21. Metzger, M.B., Pruneda, J.N., Klevit, R.E. and Weissman, A.M. (2014) RING-type E3 ligases: master manipulators of E2 ubiquitin-conjugating enzymes and ubiquitination. *Biochim. Biophys. Acta*, **1843**, 47–60.
22. Hofmann, R.M. and Pickart, C.M. (1999) Noncanonical MMS2-encoded ubiquitin-conjugating enzyme functions in assembly of novel polyubiquitin chains for DNA repair. *Cell*, **96**, 645–653.
23. Van Wijk, S.J.L., De Vries, S.J., Kemmeren, P., Huang, A., Boelens, R., Bonvin, A.M.J.J. and Timmers, H.T.M. (2009) A comprehensive framework of E2 – RING E3 interactions of the human ubiquitin–proteasome system. *Mol. Syst. Biol.*, **5**, 1–16.
24. Markson, G., Kiel, C., Hyde, R., Brown, S., Charalabous, P., Bremm, A., Semple, J., Woodsmith, J., Duley, S., Salehi-Ashtiani, K., *et al*. (2009) Analysis of the human E2 ubiquitin conjugating enzyme protein interaction network. *Genome Res.*, **19**, 1905–1911.
25. Woodsmith, J., Jenn, R.C. and Sanderson, C.M. (2012) Systematic analysis of dimeric E3-RING interactions reveals increased combinatorial complexity in human ubiquitination networks. *Mol. Cell. Proteomics*, **11**, M111.016162.

26. Budhidarmo, R., Nakatani, Y. and Day, C.L. (2012) RINGs hold the key to ubiquitin transfer. *Trends Biochem. Sci.*, **37**, 58–65.
27. Plechanovová, A., Jaffray, E.G., McMahon, S.A., Johnson, K.A., Navrátilová, I., Naismith, J.H. and Hay, R.T. (2011) Mechanism of ubiquitylation by dimeric RING ligase RNF4. *Nat. Struct. Mol. Biol.*, **18**, 1052–1059.
28. Woodsmith, J., Jenn, R.C. and Sanderson, C.M. (2012) Systematic analysis of dimeric E3-RING interactions reveals increased combinatorial complexity in human ubiquitination networks. *Mol. Cell. Proteomics*, **11**, M111.016162–M111.016162.
29. Husnjak, K. and Dikic, I. (2012) Ubiquitin-binding proteins: decoders of ubiquitin-mediated cellular functions. *Annu. Rev. Biochem.*, **81**, 291–322.
30. Swatek, K.N. and Komander, D. (2016) Ubiquitin modifications. *Cell Res.*, **26**, 399–422.
31. Guo, Y., Bian, W., Zhang, Y. and Li, H. (2016) Expression in Escherichia coli, purification and characterization of LRSAM1, a LRR and RING domain E3 ubiquitin ligase. *Protein Expr. Purif*, 10.1016/j.pep.2016.05.002.
32. Mukhopadhyay, D. and Riezman, H. (2007) Proteasome-independent functions of ubiquitin in endocytosis and signaling. *Science*, **315**, 201–205.
33. Ylikallio, E., Pöyhönen, R., Zimon, M., De Vriendt, E., Hilander, T., Paetau, A., Jordanova, A., Lönnqvist, T. and Tyynismaa, H. (2013) Deficiency of the E3 ubiquitin ligase TRIM2 in early-onset axonal neuropathy. *Hum. Mol. Genet.*, **22**, 2975–2983.
34. Tang, B., Seredenina, T., Coppola, G., Kuhn, A., Geschwind, D.H., Luthi-Carter, R. and Thomas, E.A. (2011) Gene expression profiling of R6/2 transgenic mice with different CAG repeat lengths reveals genes associated with disease onset and progression in Huntington's disease. *Neurobiol. Dis.*, **42**, 459–467.
35. Kitada, T., Asakawa, S., Hattori, N., Matsumine, H., Yamamura, Y., Minoshima, S., Yokochi, M., Mizuno, Y. and Shimizu, N. (1998) Mutations in the parkin gene cause autosomal recessive juvenile parkinsonism. *Nature*, **392**, 605–608.
36. Hattori, N. and Mizuno, Y. (2004) Pathogenetic mechanisms of parkin in Parkinson's disease. *Lancet*, **364**, 722–724.
37. Tan, E.-K. and Skipper, L.M. (2007) Pathogenic mutations in Parkinson disease. *Hum. Mutat.*, **28**, 641–653.
38. Lim, G.G.Y., Chew, K.C.M., Ng, X.-H., Henry-Basil, A., Sim, R.W.X., Tan, J.M.M., Chai, C. and Lim, K.-L. (2013) Proteasome inhibition promotes Parkin-Ubc13 interaction and lysine 63-linked ubiquitination. *PLoS One*, **8**, e73235.
39. Aerts, M.B., Weterman, M.A.J., Quadri, M., Schelhaas, H.J., Bloem, B.R., Esselink, R.A., Baas, F., Bonifati, V. and van de Warrenburg, B.P. (2016) A LRSAM1 mutation links Charcot-Marie-Tooth type 2 to Parkinson's disease. *Ann. Clin. Transl. Neurol.*, **3**, 146–149.